
EFDA–JET–CP(04)07-46

E.R. Solano, S. Jachmich, F. Villone, N. Hawkes, Y. Corre, A. Loarte, R.A. Pitts,
K. Guenther, A. Korotkov, M. Stamp, P. Andrew, J. Conboy, A. Cenedese,
M. Kempenaars, T. Bolzonella, E. Rachlew, G.F. Matthews,
and JET EFDA Contributors

ELMs, Strike Point Jumps and SOL Currents

ELMs, Strike Point Jumps and SOL Currents

E.R. Solano¹, S. Jachmich², F. Villone³, N. Hawkes⁴, Y. Corre⁵, A. Loarte⁶,
R.A. Pitts⁷, K. Guenther⁴, A. Korotkov⁴, M. Stamp⁴, P. Andrew⁴, J. Conboy⁴, A.
Cenedese⁸, M. Kempenaars⁹, T. Bolzonella¹⁰, E. Rachlew¹¹, G.F. Matthews⁴,
and JET EFDA Contributors*

¹*Asociación Euratom/CIEMAT para Fusión, Madrid, Spain*

²*ERM/KMS-LPP, Association EURATOM-Belgian State, Brussels, Belgium*

³*Università di Cassino, Assoc. EURATOM/ENEA/CREATE, DAEIMI, Cassino, Italy*

⁴*EURATOM-UKAEA Fusion Association, Culham Science Centre, Abingdon, U.K.*

⁵*Euratom-CEA Association, CEA-Cadarache, 13108, St Paul lez Durance, France*

⁶*EFDA Close Support Unit, MPI fur Plasmaphysik, Garching, Germany*

⁷*CRPP, Ass. EURATOM-Confédération Suisse, EPFL, 1015 Lausanne, Switzerland.*

⁸*Consorzio RFX, Associazione Euratom-ENEA sulla Fusione, Padova, Italy*

⁹*FOM-Rijnhuizen, Ass. Euratom-FOM, TEC, PO Box 1207, 3430 BE Nieuwegein, NL*

¹⁰*D.I.E., Università di Padova, Via Gradenigo 6/A, I-35131 Padova, Italy*

¹¹*Euratom-VR Association, Dept of Physics, KTH, 10691 Stockholm, Sweden*

** See annex of J. Pamela et al, "Overview of JET Results ",*

(Proc.20th IAEA Fusion Energy Conference, Vilamoura, Portugal (2004).

“This document is intended for publication in the open literature. It is made available on the understanding that it may not be further circulated and extracts or references may not be published prior to publication of the original when applicable, or without the consent of the Publications Officer, EFDA, Culham Science Centre, Abingdon, Oxon, OX14 3DB, UK.”

“Enquiries about Copyright and reproduction should be addressed to the Publications Officer, EFDA, Culham Science Centre, Abingdon, Oxon, OX14 3DB, UK.”

ABSTRACT.

Plasma equilibria before and after ELMs in JET are investigated. ELMs could be associated with fragile equilibria and separatrix instabilities: previously closed field lines would open up, releasing plasma current and leading to the formation of a new, smaller separatrix. This model could explain experimental observations of sudden jumps and shifts in strike point positions. Novel instability mechanisms are discussed to explain the large transient jumps observed in the strike point position: positive X-point instability, due to positive toroidal current density at the X-point and diamagnetic instability, due to negative inboard toroidal current density.

1. THEORETICAL BACKGROUND: PLASMA EQUILIBRIUM BEFORE THE ELM

Plasma force balance in a magnetic confinement device with closed field lines is given by the equation:

$$\vec{j} \times \vec{B} = \nabla p \quad (1)$$

where j is the total current density, B the magnetic field and p the pressure. In tokamak equilibrium, the pressure is usually considered as a monotonic function of Ψ , the poloidal magnetic flux per radian, $p = p(\Psi)$, so the pressure gradient is $\nabla p = p' \nabla \Psi$.

Assuming nested flux surfaces and toroidal symmetry, equation (1) leads to the Grad-Shafranov equation as a description of plasma equilibrium in a tokamak:

$$\frac{1}{\mu_0 R} \left(R \frac{\delta}{\delta R} \frac{1}{R} \frac{\delta \Psi}{\delta R} + \frac{\delta^2 \Psi}{\delta Z^2} \right) + \left(R p' + \frac{(F^2)'}{2\mu_0 R} \right) = 0 \quad (2)$$

In (2) the first term is a linear operator acting on Ψ , $L(\Psi)$. The second parenthesis is the toroidal current density,

$$j_{toroidal} = R p'(\Psi) + (F(\Psi)^2)' / (2R\mu_0) \quad (3)$$

which can be considered as a non-linear operator, J , acting on Ψ via the Ψ dependency of p' and FF' . (R, Z, ζ) are cylindrical coordinates; Ψ is the poloidal magnetic flux per radian, measured outwards from the plasma magnetic axis; the prime indicates derivative with respect to Ψ ; F is the toroidal magnetic field flux function.

Equilibrium reconstruction of the pre-ELM state is heavily influenced by how the large outboard pressure gradient is represented, usually observed in well developed H-mode plasmas with type I ELMs. A large pressure gradient can be associated either with a large $p' = dp/d\Psi$, or with large $\nabla \Psi$. The choice is typically determined by internal magnetic or kinetic constraints. In JET ELMy H-modes, typically p' is typically non-zero at the outer equator across the separatrix. As a consequence, the toroidal current density, $j_{toroidal}$, is not necessarily zero at the X-point, while $j_{poloidal}$ must be zero. We will return to this point in section 3, as it can lead to instability.

As a further consequence of the large edge ∇p and p' , there is also a large diamagnetic current: the poloidal current density is typically diamagnetic at the plasma edge and F' has opposite sign to p' in equation (3). In a sufficiently diamagnetic plasma, the inboard edge toroidal density can be negative since the F' contribution to the toroidal current density is amplified by $1/R$, while p' is multiplied by R . This is a typical feature of H-mode plasmas [1].

Allowing for non-zero currents at the separatrix, internal magnetic field measurements from polarimetry and Motional Stark effect and external magnetic measurements have been used in JET to reconstruct a pre-ELM equilibrium, corresponding to the event described in section 2. Its current density profiles are illustrated in Fig.1, plotted at the plasma equator. Edge diamagnetism is a robust feature of the reconstruction, while negative inboard j_{toroidal} is not always present, probably due to insufficient diagnostic constraints.

If local equilibrium is lost somewhere inside the separatrix, that flux surface might “break”, and the previously closed flux surfaces outside it would open. Particles, energy and current would flow along these newly opened field lines and be rapidly lost. We describe such a process as a peeling of previously closed flux surfaces. The sudden loss of current from inside the separatrix leads to the formation of a new, smaller separatrix, with displaced X and strike points (since the divertor and shape control coil currents cannot change on the ELM timescale). The strike points would move towards the plasma centre (upwards in JET vertical target plasmas).

Additionally, at the inboard plasma equator, the loss of counter-current would lead to an increase in the magnitude of the local vertical field. Outboard, the magnitude of the local vertical field would decrease, as positive co-current is lost. Changes in local magnetic measurements at ELMs were first explained as an inboard plasma displacement [2]. They have also been seen in JET, as shown in Fig.2. The sudden changes are consistent with our peeling model, if the diamagnetic counter current is properly taken into account. -

2. TYPE I ELMs IN JET: STRIKE POINT MOVEMENTS.

Specific experiments have been designed and executed to investigate strike point movement during ELMs in JET [3, 4]. To maximize diagnostic sensitivity, plasmas were designed with infrequent ELMs and strike point positions were optimised for good InfraRed (IR) viewing and divertor target Langmuir Probe (LP) array coverage. Discharges yielding the best data had 2.4MA of plasma current, toroidal field of 2.4T, 15MW of neutral beam injection heating and no gas-puff during the heating phase. They are characterised by 1 Hz compound ELMs with a diamagnetic energy drop of order $\Delta W_{\text{dia}} = 500\text{kJ}$. The same general behaviour of the strike points has been observed in a variety of other discharge types.

Figures 3 and 4 illustrate typical observations of strike movements at a compound ELM in JET. The contour plots of tile surface temperature (Figs. 3b, 4b) and ion saturation current (Figs. 3c, 4c) clearly show both the pre-ELM position and how subsequent small ELMs arrive at a higher location, about 2cm above the pre-ELM location. The strike points have shifted after the leading ELM.

Later, after the end of the ELM phase, the strike points return to the pre-ELM position. On a faster time scale, approaching the diagnostic time resolution limit, much larger strike jumps are consistently observed, associated with the leading ELM. Note in Fig. 3d and 4d that the LP array detects sudden large strike point position jumps, about 20cm inboard and 7 cm outboard in 100 μ s (the time resolution of the diagnostic). The inboard observation of the sudden jump is supported in part by the IR diagnostic, in the form of a bright flash visible 12cm above the pre-ELM position inboard. This transient surface heating disappears in less than 65 μ s (Fig 3b). The IR response to such transients is enhanced at the inboard tiles by the presence of a thin layer of co-deposited material with poor thermal conductivity which reacts quickly to the incoming ELM power. On the outboard tiles, the IR contours in Fig. 4b show a new strike position, but the tile remains hot for some time even after power ceases to arrive at the pre-ELM position, as shown in Fig. 4d, where the position of the hottest pixel is plotted.

Are strike shifts associated with global plasma movements? Not in this case [3]. The vertical position of the centre of SXR emission has a sudden (<100 μ s) 7mm downshift, followed by a return to the previous position in < 100 μ s, and a slow upward drift of 1cm in 10ms. This fast downshift of the centre coincides in time with the large upward jump of the strikes (LPs), and so cannot be due to an upward plasma movement. Further evidence of plasma edge erosion, rather than plasma movement, comes from edge density measurements, obtained with a Li beam along a vertical line at the plasma top (100ms time resolution). After each ELM, loss of density is observed from the top edge surfaces. The line integrated density is measured along 3 interferometre vertical lines located inboard and outboard of the magnetic axis and at the outer edge (up to 1ms resolution). A simultaneous sudden drop in all 3 line integrals indicates that the fast density loss observed by the Li beam is not due to an in-out movement of the plasma centre.

3. MODELLING PLASMA PEELING

Starting from the equilibrium depicted in Fig.1, a linearized plasma response model [5] is used to compute a new equilibrium by peeling surfaces outside a given normalised Ψ value, accounting for induced currents in passive structures (large in sudden events in JET). The eddy currents can be considered, in part, as a representation of the currents flowing in the Scrape-Off Layer (SOL), which transiently oppose the initial flux changes. Peeling flux surfaces outside of $\Psi_N = 0.97$ results in the loss of 46kA of toroidal current, a loss of diamagnetic energy $\Delta W_{\text{dia}} \sim 0.5\text{MJ}$, and upward strike shifts of 4cm inboard, 3cm outboard.

A breakdown of the various contributions to the total system energy before and after the ELM is presented in Table 1. It is interesting that due to the loss of diamagnetic current from the plasma edge, the largest changes are an exchange of the toroidal field energies in plasma and vacuum regions. The drop in kinetic pressure and poloidal field energy is compensated in part by the increase in toroidal plasma field energy. The final state has a 0.5MJ drop in plasma kinetic energy, approximately consistent with the experimental observation of ΔW_{dia} . As the peeled state has lower

energy than the pre-ELM state, peeling of flux surfaces can be a physically allowable transition. The pre and post-ELM strike positions of the reconstructed equilibrium are compared with LP measurements in Table 2. They show good agreement with LP measurements outboard (where more measurement constraints are available), but not inboard. Alternative reconstructed equilibria, adding edge pressure constraints, can strongly reduce the discrepancy in the pre-ELM inboard strike position, but choosing amongst the various alternatives is non-trivial. Additional experimental constraints from observed MHD modes will be added to the reconstruction. For now, we present the results of the initial reconstruction simply to gauge the effects of peeling, while admitting that model results may depend strongly on current profile details of the pre-ELM state that cannot (yet) be ascertained.

How about the transient strike jumps observed? One possible explanation of the large sudden jumps is associated with the non-zero toroidal current density at the X-point. As the separatrix breaks, the X-point co-current carrying flux tube is displaced towards the private flux region [6]. There it will be accelerated further towards the divertor coils since the attractive $\mathbf{j} \times \mathbf{B}$ force from the core plasma decreases while the force from the divertor coils increases. Transiently, a new X-point would form, closer to the core plasma, when the externally imposed diverting fields are increased by the field produced from the detached current carrying flux tube. This situation has been modelled by adding the toroidal lost plasma current, 40kA, to the divertor coils, to simulate the presence of currents flowing transiently in the SOL, including the private flux region. Again, results are shown in Table 2 (first 2 rows), next to LP measurements, and agreement is fairly good for outboard strike movements.

How long will the transient last? In the private flux region the connection length is 5m, so the current would dissipate in about $10\mu\text{s}$ (assuming 1.5keV ions to compute sound speed). In the main SOL the connection lengths from the midplane are 20m, so those SOL currents would dissipate in $50\mu\text{s}$, or faster if current filaments are displaced radially. The post-ELM state would therefore be reached in $50\mu\text{s}$ or less. This is consistent with the fact that the sudden large strike jumps are only seen in 1 time point of the 10kHz LP data [4], and only occasionally with the IR camera (1 frame = 3ms).

Here we should mention that the toroidal current at the X-point might itself trigger the ELM. If the toroidal current density increases in magnitude as the X-point is approached, a position instability of the X-point current filament could be responsible for breaking of the separatrix. A simple magneto-static model of this X-point instability was presented in [6] simulating a double null plasma with current filaments. The evolving pre-ELM state can be described by displacing 2 current filaments (each carrying 2% of the 2.4 MA of plasma current) towards the X-points, from the plasma centre. Results are presented in the bottom row of Table 2. As the filaments are swept towards the divertor coils, but still inside the main separatrix, the strikes sweep down to -1.66m . In the transient state, while current flows in the private flux regions, up to 6cm upward strike jumps can be explained. Whether the 15 cm inboard strike jumps could be explained refining any of our models is less clear.

For a given plasma configuration, increasing β_{poloidal} and triangularity increases diamagnetism

and reduces the toroidal current density at the X-point, increasing the positional stability of the current-carrying X-point. Equally, higher edge densities lead to colder edges, with less current. Type II ELM behaviour, usually associated with high triangularities and densities (cold edge), could be associated with more stable X-points.

Besides affecting the stability of the current carrying X-point, diamagnetism may itself provide an alternate instability mechanism contributing to the ELM trigger. As described in Section 1, as the pressure gradient increases, diamagnetism drives the inboard j_{toroidal} more negative, while the outboard j_{toroidal} increases with the increase in p' . The repulsion between filaments with opposing currents (poloidal and toroidal) might render the equilibrium fragile on the high field side. Measurements of poloidal magnetic field (Fig. 2) at the inboard and outboard plasma equator are consistent with the growth of counter j_{toroidal} inboard and co-current outboard before the ELMs, and the loss of such edge currents after the ELM.'

4. EQUILIBRIUM CRITICALITY ANALYSIS

Considering equation (2) as a non-linear partial differential equation, we can study its criticality [7]: the identification of situations such that the number of solutions of the equation changes under a small perturbation of the equation. Criticality can be identified in the Grad-Shafranov equation by searching for regions of the plasma where the operator equation acting on the solution $\Psi(R,Z)$

$$\partial J / \partial \Psi = J \Psi \quad (4)$$

is locally satisfied.

That study led us to conjecture that the formation of a transport barrier corresponds to the appearance of a new solution branch of equation (2) with a locally diamagnetic region. The equilibrium reconstruction presented in Fig.1 does display diamagnetism in the edge barrier region, in agreement with this conjecture. Evidence for a possible association between diamagnetism and the L-H transition can be seen in Fig.2, where we show the local poloidal magnetic field inboard and outboard of the plasma, at the plasma equator. Clearly there is a break in the time derivative at the L to H transition, as would be expected if diamagnetism increased at this point.

Conversely, we conjecture that in critical situations, a given equilibrium solution may be locally fragile. From there the plasma could peel. An ELM could be the consequence of such equilibrium fragility. The particular equilibrium depicted in Fig.1 does not satisfy the criticality condition (4) at the equatorial edges or the X-point: this equilibrium is not fragile. Minor modifications of the edge current profiles do produce nearby equilibria that satisfy the criticality condition. In particular the addition of pre-ELM edge pressure measurements near the X-point does lead to an equilibrium that is fragile at $\Psi_N = 0.95$ near the X-point. Regrettably, given our present equilibrium reconstruction capabilities we can say that equilibrium fragility (at the X-point, inboard or outboard equator) are all possible reasons for the ELM, but stronger statements cannot be made at the moment.

CONCLUSIONS

The study of strike point positions in JET, before and after ELMs, complements other profile and magnetic information. The experimental data clearly shows that strike points are shifted several centimetres upward soon after an ELM event (about 100 μ s after the D_α rise). During the transient phase, much larger upward displacements are observed.

We have explored the possibility that ELMs are associated with instabilities that break previously closed flux surfaces, including the separatrix. The experimental evidence does support such a “peeling” model of type I ELMs. During the transient phase, an overshoot of the strike shifts could be due (in part) to the presence of toroidal currents in the private flux region, transiently driving the strike points further up.

Two novel instability mechanisms were considered, both associated with edge currents: the X-point instability and the diamagnetic instability. Details of the pre-ELM equilibrium reconstruction are still insufficiently quantified for reliable MHD studies in this case. Regardless of which instability mechanism triggers the ELM, the evidence for peeling remains. Therefore the ELM is unlikely to be associated to a simple reduction of pressure gradients in a fixed equilibrium. A complete model must take into account the new flux surface geometry, with a reduced separatrix.

ACKNOWLEDGEMENTS:

This work has been conducted under the European Fusion Development Agreement, and has been funded in part by a Ramón y Cajal grant from the MEC, Spain.

REFERENCES

- [1]. Lao, L. L. , Nuclear Fusion vol.30 no.6 June 1990 p.1035.
- [2]. Von Goeler, S., *ibid.*, p.395
- [3]. Solano, E. R., Villone, F., Hawkes, N. et al., “Current Loss and Strike Point Movement During ELMs in JET”, 30th Conf. on Control. Fusion and Plasma Physics, St Petersburg, Russia, July 7–11, 2003, Europhysics Conf. Abs Vol. 26B, 01.106, http://epsppd.epfl.ch/StPetersburg/PDF/P1_106.PDF
- [4]. Solano, E. R., Jachmich, S., Villone, F., et al., “ELMs and Strike Point Jumps”, 16th Conf. on Plasma Surface Interactions in Controlled Fusion Devices, Portland Maine, U.S.A, May 24–28, 2004, to be published in Jour. Nucl. Mater.
- [5]. Albanese, R., Villone, F., Nuclear Fusion, **38**, 723- 738 (1998)
- [6]. Solano, E. R., Villone, F., “Separatrix instability and ELMs”, 31st Conf. on Plasma Physics, London, 28 June-2nd July 2004, Imperial College, London. Europhysics Conf. Abs Vol. 28G, 01.171.”
- [7]. Solano, E.R., Plasma Phys. Control. Fusion, Vol.46, No.3, March 2004, p.L7.

| Energy (MJ) | before ELM | % | after ELM | % of total | Change (MJ) |
|-------------------|------------|---------|-----------|------------|--------------|
| Pressure : | 4.23 | 0.06% | 3.70 | 0.05% | -0.53 |
| Magnetic: | | | | | |
| Plasma | | | | | |
| Poloidal | 4.13 | 0.06% | 4.08 | 0.06% | -0.04 |
| Toroidal | 180.6 | 2.44% | 181.9 | 2.46% | +1.30 |
| Vacuum | | | | | |
| Poloidal | 34.9 | 0.47% | 34.7 | 0.47% | -0.16 |
| Toroidal | 6710. | 90.61% | 6709. | 90.60% | -0.98 |
| Iron Core | | | | | |
| Poloidal | 36.3 | 0.49% | 36.3 | 0.49% | 0 |
| Conductors | | | | | |
| Poloidal | 20.4 | 0.28% | 20.4 | 0.28% | -0.02 |
| Toroidal | 415 | 5.61% | 415 | 5.61% | 0 |
| Total | 7405 | 100.00% | 7404 | 100.00% | -0.44 |

Table 1. Computed contributions to system energy in model pre-ELM equilibrium for Pulse No:58837, and with plasma peeled off from $\Psi_N = 0.97$.

| Strike point height Z(m) | before ELM | | ELM transient | | Post-ELM | | ΔZ (m) | |
|-----------------------------|----------------|-------|----------------|-------|----------|-------|----------------|-------|
| | LP | Eq. | LP | Eq. | LP | Eq. | LP | Eq. |
| Inner strike Z | -1.63 | -1.69 | -1.40 | -1.63 | -1.61 | -1.65 | +0.02 | +0.04 |
| Outer strike Z | -1.64 | -1.65 | -1.57 | -1.57 | -1.62 | -1.62 | +0.02 | +0.03 |
| Filament model | -1.62 to -1.66 | | -1.66 to -1.61 | | -1.61 | | +0.01 to +0.05 | |

Table 2. Z(m) position of strike points, inboard and outboard, comparing LP data and models (filament model in bottom row). $\Delta Z = Z_{post-ELM} - Z_{pre-ELM}$. LP spacing of order 0.02-0.05m, finest resolution near -1.63m.

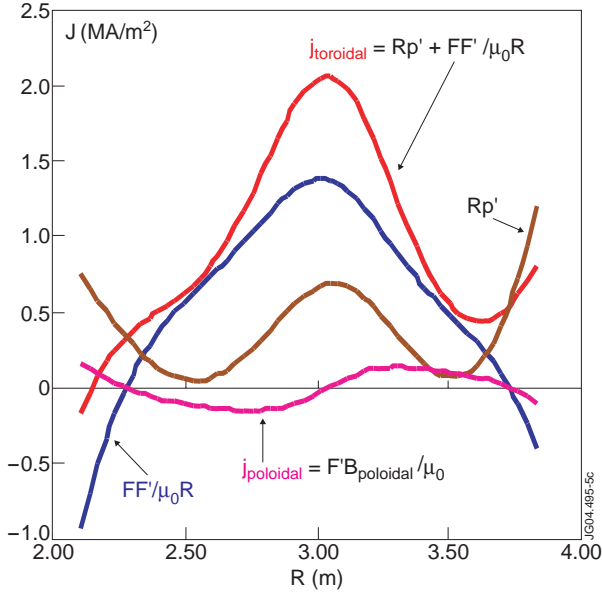


Figure 1: Current densities for JET Pulse No: 58837 at 21.4s, along plasma equator, just before an ELM. Note inboard negative toroidal current due to diamagnetism.

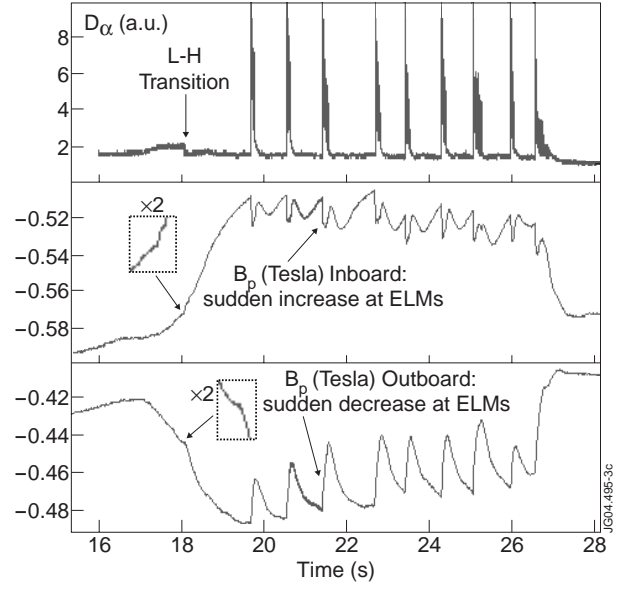


Figure 2: D_α and local poloidal magnetic fields in-board and outboard. JET Pulse No: 58837. Note changes at L-H transition and ELMs.

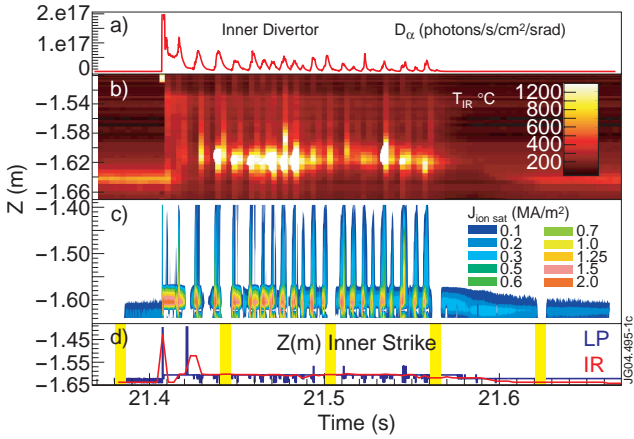


Figure 3: ELM characteristics, in inner divertor leg: a) D_α signal; b) contours of tile temperature T (Celsius) from IR, vs. height at target tile¹; c) contours of ion saturation current (A/m^2), from LPs; vs. probe height along target tile; d) strike position^{1,2}, as maximum of ion saturation current (LP, blue) and maximum T (IR, red).

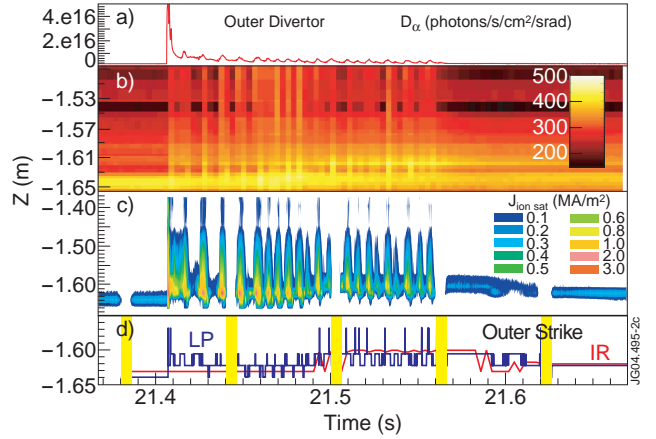


Figure 4: ELM characteristics, in outer divertor leg: same as above^{1,2}.

¹ Z_{IR} and $time_{IR}$ manually shifted to match Z_{LP} during pre-ELM phase and D_α spike time.

² Periodic voltage reversal is applied to LPs to avoid arcs. During this time, marked with yellow bars, strike positions are not well identified by LPs